International Journal of Nanomedicine

Dovepress
open access to scientific and medical research

Open Access Full Text Article

ORIGINAL RESEARCH

# Self-assembled poly(ε-caprolactone)-*g*-chondroitin sulfate copolymers as an intracellular doxorubicin delivery carrier against lung cancer cells

This article was published in the following Dove Press journal:
International Journal of Nanomedicine
31 July 2012
Number of times this article has been viewed

Yue-Jin Lin[1]
Yu-Sheng Liu[1]
Hsin-Hwa Yeh[1]
Tian-Lu Cheng[2]
Li-Fang Wang[1]

[1]Department of Medicinal and Applied Chemistry, [2]Department of Biomedical Science and Environmental Biology, College of Life Science, Kaohsiung Medical University, Kaohsiung, Taiwan

**Abstract:** The aim of this study was to utilize self-assembled polycaprolactone (PCL)-grafted chondroitin sulfate (CS) as an anticancer drug carrier. We separately introduced double bonds to the hydrophobic PCL and the hydrophilic CS. The modified PCL was reacted with the modified CS through a radical reaction (CSMA-g-PCL). The copolymer without doxorubicin (DOX) was noncytotoxic in CRL-5802 and NCI-H358 cells at a concentration ranging from 5–1000 μg/mL and DOX-loaded CSMA-g-PCL (Micelle DOX) had the lowest inhibitory concentration of 50% cell growth values against the NCI-H358 cells among test samples. The cellular uptake of Micelle DOX into the cells was confirmed by flow cytometric data and confocal laser scanning microscopic images. The in vivo tumor-targeting efficacy of Micelle DOX was realized using an NCI-H358 xenograft nude mouse model. The mice administered with Micelle DOX showed suppressed growth of the NCI-H358 lung tumor compared with those administered with phosphate-buffered saline and free DOX.

**Keywords:** chondroitin sulfate, poly(ε-caprolactone), amphiphilic copolymers, micelles, cellular uptake

## Introduction

Self-assembly of amphiphilic copolymers in aqueous media generally results in aggregates of core-shell structures. Great control of micelle shapes and sizes has an important effect on the functions and properties of drug delivery systems. Using micelles to solubilize hydrophobic agents and to improve pharmacokinetics provides a promising bioengineering platform for chemotherapy in treating cancer diseases.[1,2]

Micelles based on biodegradable polycaprolactone (PCL) have been extensively investigated using poly(ethylene glycol), termed PEG, as a hydrophilic counter polymer (PCL-PEG) to prevent recognition from the reticuloendothelial system (RES).[3–5] Polysaccharides have been developed in parallel to PEG-decorated ones, not only because of the ability to prevent recognition from the RES, but also because of the presence of derivable groups on molecular chains, which enrich the versatility of drug carriers in terms of categories and functions.[6] For example, PCL and dextran (PCL-DEX) nanoparticles have been synthesized and studied for their stability and interactions with biological systems.[7–10] Polymeric micelles obtained by self-assembly of hyaluronic acid–polyethylene glycol–polycaprolactone (HA–PEG–PCL),[11] HA-grafted polylactic acid and PEG,[12] HA-grafted poly(glycolic-co-lactic acid),[13] and stearate-grafted dextran polymers[14] have all been used to prepare a targeted delivery system of doxorubicin (DOX) to tumors.

Correspondence: Li-Fang Wang
Kaohsiung Medical University, School of Life Science, 100, Shih-Chuan 1st Rd, Kaohsiung City 807, Taiwan
Tel +11 886 7312 1101 ext 2217
Fax +11 886 7312 5339
Email lfwang@kmu.edu.tw

Chondroitin sulfate (CS) is a natural glycosaminoglycan widely distributed in the human organism. It binds endogenous proteins with different functional properties such as growth factors, adhesion molecules or enzymes, which regulate the human immune system.[15] CS has a similar chemical structure to HA, except there are sulfated groups in the C4 or C6 position. The negative charges of CS prevent micelle aggregation. CS has many promising properties such as biocompatibility, biodegradability, anti-inflammatory, and as a good structure/disease-modifying antiosteoarthritis drug (S/DMOAD).[16]

Our previous study successfully introduced the methacrylate groups to CS (CSMA) for preparing a pH-sensitive hydrogel.[17] The vinyl groups on CSMA could be used to react with PCL end-capped double bonds to produce a graft copolymer (CSMA-*g*-PCL). Various amounts of PCL were grafted onto CSMA with three different degrees of methacrylation. The chemical–physical properties and morphologies of the CSMA-*g*-PCL were systematically characterized.[18,19] PCL is one of the semicrystalline linear restorable aliphatic polyesters. Thus, CSMA-*g*-PCL is subject to biodegradation due to the susceptibility of its aliphatic ester and sugar linkages to hydrolysis.

In this contribution, an optimized composition of PCL on CSMA-*g*-PCL was synthesized via a free radical reaction. It appears worthwhile to use PCL as a core and CSMA as a shell because CS is a highly water soluble anionic polysaccharide and this prevents recognition from the RES. PCL is a US Food and Drug Administration-approved nontoxic polyester, which is highly hydrophobic. The greater discrepancy between the hydrophilic CS and the hydrophobic PCL results in self-assembly with a lower critical micelle concentration (CMC) value. The lower CMC value benefits the stabilization of nanoparticles in the bloodstream. The optimized condition was adapted to prepare the stable CSMA-g-PCL micelle in a large quantity and a model drug, DOX, was loaded. The cell-killing potency was tested in five non-small-cell lung cancer cells (NSCLC). The two most potent cell lines, CRL-5802 and NCI-H358, were selected for detailed cell viability studies when exposed to free DOX and Micelle DOX. The cellular uptake of DOX was realized using a flow cytometer and a confocal laser scanning microscope (CLSM). The antitumor activity of free DOX and Micelle DOX against the NCI-H358 tumor was tested.

# Materials and method

## Materials

Sodium chondroitin sulfate was purchased from Tohoku Miyagi Pharmaceutical Co, Ltd (Tokyo, Japan). Methacrylic anhydride and acryloyl chloride were purchased from Alfa Aesar (Ward Hill, MA) and used as received. Pyrene, ε-caprolactone, 2,2′-azobisisobutyronitrile (AIBN), and 1,1′-carbonyldiimidazole (CDI, 97%) were purchased from Acros (Fairlawn, NJ). DOX was purchased from Aldrich (St Louis, MO) and Lipo-DOX® was acquired from TTY Biopharm (Taipei, Taiwan). Fetal bovine serum (FBS) was from Biological Industries (Beit Haemek, Israel). Potassium dihydrogen phosphate, disodium hydrogen phosphate, glycine, boric acid, and hydrochloric acid were purchased from Fluka (Buchs, Switzerland) and used for buffer preparation. 3-(4,5-Dimethyl-thiazol-2yl)-2,5-diphenyl-tetrazolium bromide (MTT) was from MP Biomedicals (Eschwege, Germany) and Dulbecco's modified Eagle's medium (DMEM) was from Gibco BRL (Paris, France). All other unstated chemicals were purchased from Sigma Chemical (St Louis, MO) and used without further purification.

## Synthesis of methacrylated chondroitin sulfate (CSMA) and poly(ε-caprolactone) end-capped with the acrylated group (MeO-PCL-Ac)

The synthesis of CSMA was performed according to our previous report.[17] The degree of methacrylation on CS was controlled at 70%. The synthesis of MeO-PCL-Ac was performed as described previously.[19]

## Synthesis of CSMA-*g*-PCL copolymer

One hundred milligrams of MeO-PCL-Ac in 100 mL of dimethylsulfoxide (DMSO) was dissolved at 60°C. One hundred milligrams of CSMA in 1 mL of DD water was gradually added to the above solution in an argon atmosphere. One wt% AIBN in DMSO relative to the total weight of MeO-PCL-Ac and CSMA was added into the reaction mixture, which was continuously stirred for 8 hours at 60°C. After cooling to room temperature, the reaction mixture was poured into a dialysis membrane (MWCO 6000–8000, Spectra/Pro 7; Spectrum Laboratories Inc, Rancho Dominguez, CA) and dialyzed against DD water, which was changed every 3–6 hours for 2 days to remove DMSO and other initiator residues. The aqueous solution in the dialysis tube was removed and freeze-dried. The resulting product was further washed thrice with ethyl acetate to remove MeO-PCL-Ac residues. Next, the precipitate was dissolved in DD water and centrifuged for 5 minutes at 12,000 rpm. The aqueous solution was removed and freeze-dried. The yield of the final product was approximately 55% and the product was stored at −20°C for further use.

## Characterization of CSMA-g-PCL

The Fourier transform infrared (FTIR) spectra were obtained on a Perkin Elmer 2000 (Perkin Elmer, NJ) spectrometer. Dried samples were pressed with potassium bromide (KBr) powder into pellets. Sixty-four scans were signal-averaged in the range from 4000 to 400 $cm^{-1}$ at a resolution of 4 $cm^{-1}$. The nuclear magnetic resonance ($^1$H-NMR) spectrum was recorded on a Gemini-200 spectrometer (Varian, CA) using DMSO-$d_6$ as a solvent. Fluorescence spectra were recorded on a Cary Eclipse fluorescence spectrophotometer (Cary, Varian, CA). Pyrene was used as a fluorescence probe. Pyrene excitation spectra were recorded using an emission wavelength at 390 nm. The emission and excitation slit widths were set at 2.5 and 2.5 nm, respectively. A CMC value was determined from the ratios of pyrene intensities at 339 and 336 nm and calculated from the intersection of two tangent plots of $I_{339}/I_{336}$ versus the log concentrations of the polymers.[18]

The hydrodynamic diameters of micelles were measured using a dynamic light-scattering (DLS) zetasizer (3000HS; Malvern Instruments, Malvern, UK). The samples were measured in DD water at a concentration of 0.1 mg/mL and 37°C after filtering with 0.45 μm disc filter. The particle size and morphology of the micelles were also visualized using a transmission electron microscope (TEM, JEM-2000 EXII; JEOL, Tokyo, Japan). A carbon-coated 200 mesh copper specimen grid (Agar Scientific Ltd, Essex, UK) was glow-discharged for 1.5 minutes. One drop of the micelles was deposited on the grid and left to stand for 2 minutes, and then any excess fluid was removed with a filter paper. The grids were allowed to dry for 2 days at room temperature (RT) and examined with an electron microscope.

## Preparation and release of DOX-loaded CSMA-g-PCL (Micelle DOX)

A base form of DOX was prepared by dissolving 10 mg of DOX-HCl in 2.5 mL of DMSO containing three molar excess of triethylamine (TEA). The DOX base solution was slowly added into the CSMA-g-PCL solution of 1 mg/mL of DMSO and the weight ratio between DOX and CSMA-g-PCL was controlled at 1/10. The DOX-loaded CSMA-g-PCL solution was dialyzed against DD water for 24 hours (membrane cut-off MW of 1000 Da) followed by freeze-drying. To evaluate DOX loading efficiency, a dried sample was dissolved in DMSO and the absorbance was measured using a UV-Vis spectrometer at 485 nm. The DOX amount was calculated from a standard calibration curve in the concentration range from 5–100 μg/mL made of free DOX. Accordingly, IR780 was loaded for optical imaging following a similar method stated in the DOX-loaded CSMA-g-PCL without using TEA.

$$\text{Loading efficiency: } \frac{w_b}{w_c} \times 100\% \quad (1)$$

where $w_b$ are the amounts of drug in the sample; and $w_c$ is the weight of CSMA-g-PCL micelles.

The in vitro release kinetics of DOX from DOX-loaded CSMA-g-PCL (Micelle DOX) was determined in 0.1 M phosphate-buffered saline (PBS) buffers at pH 6.2 or 7.4 at 37°C. One mg of Micelle DOX was suspended in 1 mL of the above buffers. Each Eppendorf was kept in a shaker at 37°C and 150 rpm. At predetermined time intervals, four Eppendorfs were removed from the shaker and centrifuged at 12,000 rpm, 4°C for 5 min. The supernatants were collected to estimate the amount of DOX release, which was correlated to a standard calibration curve of DOX in the same buffer using a UV-Vis spectrophotometer, as mentioned above.

## Cytotoxicity

Five human non-small-cell lung cancer cell lines: CL1-5, H928, NCI-H520, NCI-H358, and CRL-5802 cells from Dr Cheng's group at Kaohsiung Medical University of Taiwan were grown and maintained in DMEM. The cell culture medium was supplemented with 10% FBS, 100 μg/mL streptomycin, and 100 U/mL penicillin at 37°C under 5% $CO_2$. Cells were seeded in 96-well tissue culture plates at a density of $3 \times 10^3$ cells per well. After 24 h, the culture medium was replaced with 100 μL of medium containing CSMA-g-PCL at a concentration of 5–1000 μg/mL or an equivalent DOX concentration in Micelle DOX of 0.01–10 μg/mL, respectively. After 24 hours, the medium was removed and the cells were washed thrice with 100 μL of 0.1 M PBS at pH 7.4. The number of viable cells was determined by estimating their mitochondrial reductase activity using the tetrazolium-based (MTT) colorimetric method.[20] The spectrophotometric absorbance of the sample was measured at 590 nm using a microplate reader (Thermo, Waltham, MA).

## Flow cytometry

NCI-H358 and CRL-5802 cells were cultured in a 75 T flask 7 days before conducting the following experiment. The cells were detached by 0.1% 1X trypsin and washed with 10 mL of 0.1 M PBS. The $3 \times 10^5$ cells were distributed into 6-well culture plates using the same medium as the MTT assay and incubated for 24 hours at 37°C. Free DOX, Lipo DOX®, or Micelle DOX were added at a DOX concentration of 0.5 μg/mL in the same culture medium and then incubated

for various time periods. The culture mediums were aspirated and the cells were washed and detached by 0.1% 1X trypsin of 1 mL per well and centrifuged at 1000 rpm for 5 minutes. The pellets were resuspended in 1 mL of 0.1 M PBS and the $1 \times 10^4$ cell counts were analyzed using an EPICS XL Flow Cytometer (Beckman Coulter, Fullerton, CA).

## Confocal laser scanning microscopy (CLSM)

NCI-H358 and CRL-5802 cells ($1 \times 10^5$ cells/well) were seeded into a 12-well culture plate in DMEM containing one glass coverslip per well and incubated for 24 hours at 37°C. The medium was removed and 2 mL of PBS (pH 7.4 and 0.2% FBS) containing an equivalent DOX concentration of 0.5 μg/mL was added into each well. The plate was then incubated for various time periods at 37°C. After incubation and several washes, the coverslips with the cells were removed, placed in empty wells, and treated with 1 mL of 3.7% formaldehyde in 0.1 M PBS for 30 minutes. The cells were treated with 1 mL/well of 0.1% Triton X-100 and incubated for 10 minutes. After three washings with 0.1 M PBS, the cells were then incubated with 0.5 mL/well of DAPI (1 μg/mL) for 5 minutes at 37°C. An Olympus Fv 500 CLSM (Tokyo, Japan) was used for cell imaging. The emission wavelength was set to 565 nm.

## Biodistribution by optical imaging

Nude mice (Balb/cAnN-Foxn1nu/CrlNarl, female) were subcutaneously injected with $6 \times 10^6$ CRL-5802 and NCI-H358 cells respectively in their right and left hind leg regions. After 14 days for tumor growth to a size of about 100 $mm^3$, an IR780-encapsulated CSMA-g-PCL was intravenously injected through the tail vein. Optical images of the tumor-bearing mice were taken using an Ultra Sensitive Molecular Imaging System (NightOWL II LB NC100; Berthold, Bad, Germany) at different time points after the injection. The tumor-bearing nude mice were anesthetized with 2.5% isoflurane before being placed into the imaging chamber and imaged at various time points after injection of the IR780-encapsulated CSMA-g-PCL. Relevant organs, tissues, and tumors were dissected from the mice and imaged immediately to determine biodistribution. Fluorescence emission was normalized to pixels per millimeter squared ($p/mm^2$).

## In vivo antitumor efficacy

The antitumor efficacy of Micelle DOX was evaluated in NCI-H358 tumor bearing mice as the aforementioned with only one tumor grafted on the right hind leg. When the tumors were approximately 150 $mm^3$, PBS, free DOX, or Micelle DOX was intravenously injected via the lateral tail vein at a single dose of 5 mg DOX/Kg animal as described previously.[21] The tumor volumes measured every 2 days were calculated as $w^2 \times l/2$, where $l$ was the largest and $w$ was the smallest diameter. On day 42, tumors were dissected from the mice and imaged immediately.

## Statistical methods

The results were reported as mean ± standard deviation. Differences between the experimental groups and the control groups were tested using Student's–Newman–Keuls test and $P < 0.05$ were considered significant.

# Results and discussion

## Preparation of initial macromers and copolymers

The ring-opening polymerization of ε–caprolactone (CL) was initiated by anhydrous methanol without using any catalysts at a high temperature of 230°C and its chemical structure was confirmed by $^1$H-NMR (Supplemental Figure S1A). Besides the characteristic peaks assigned for MeO-PCL-OH, $^1$H-NMR ($CDCl_3$, δ, ppm) spectrum for MeO-PCL-Ac appears three additional peaks at 6.35 (dd, 1.8 and 17.2 Hz, *cis* $H_2C$=CH), 6.05 (dd, 10.2 and 17.2 Hz, $H_2C$=C<u>H</u>), and 5.85(dd, 1.8 and 10.2 Hz, *trans* $H_2C$=CH), The number average molecular weight of MeO-PCL-OH calculated from MALDI-TOF was 2200 g/mole (Supplemental Figure S1B). The hydroxyl groups of MeO-PCL-OH were acrylated by reaction with a large excess of acryloyl chloride. MeO-PCL-Ac was confirmed by $^1$H-NMR (Supplemental Figure S1C). The characteristic peaks at 5.85, 6.06, and 6.35 ppm were the three protons attached on C=C double bonds. CSMA was synthesized following the method reported previously.[17] The degree of MA substitution onto CS was approximately 70% per repeating unit.

An amphiphilic copolymer combining extremely different hydrophilic and hydrophobic characteristics between CS and PCL was successfully synthesized previously.[18] A chemical reaction is shown in Scheme 1. Both CS and PCL are biodegradable and US Food and Drug Administration-approved for clinical use. The weight ratio of 1/1 between CSMA and MeO-PCL-Ac in the feed was used to prepare CSMA-g-PCL. The FTIR spectrum of CSMA-g-PCL was identified because the combinational absorption peaks were observed from CSMA and PCL (Figure 1A). The –OH stretching in the 3200–3600 $cm^{-1}$ region and the maximum signal of –CONH amide at 1646 $cm^{-1}$ were mainly

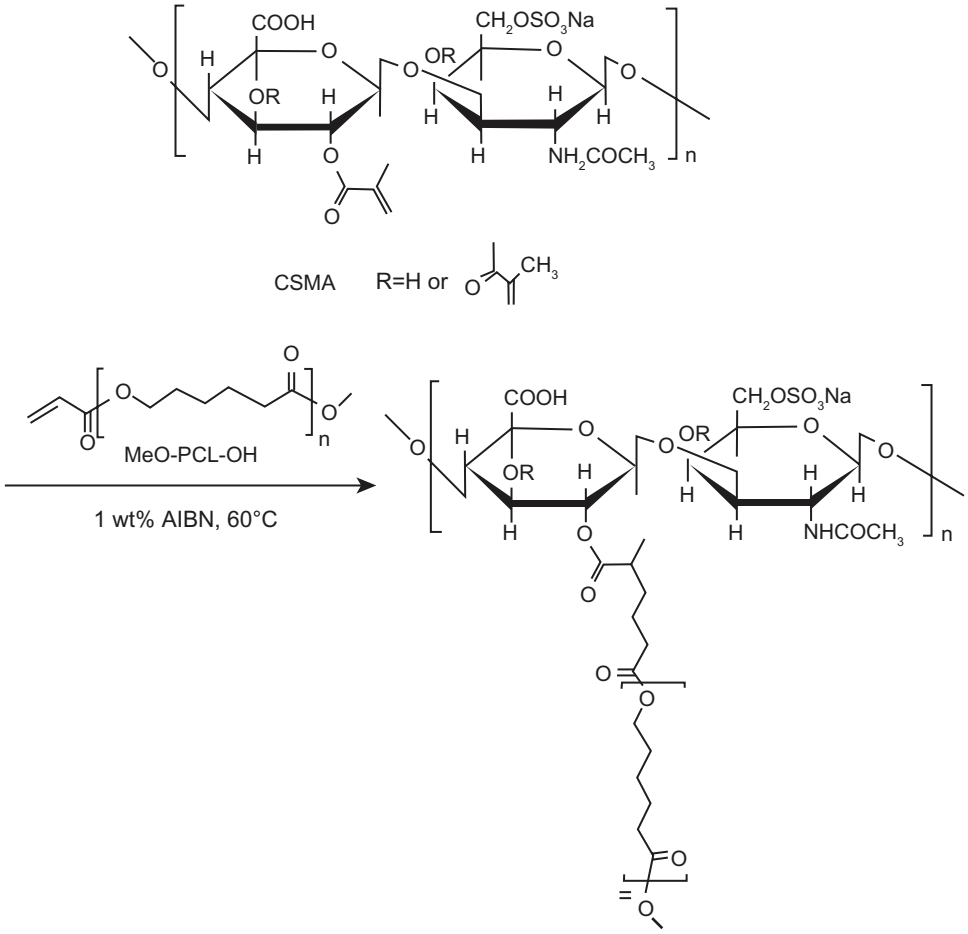


**Scheme 1** The chemical reaction of CSMA-g-PCL.
**Abbreviations:** CSMA, Methacrlyated chondroitin sulfate; MeO-PCL-OH, Methoxy-capped poly(ε-caprolactone); CSMA-g-PCL, Poly(ε-caprolactone)-g-methacrylated chondroitin sulfate; AIBN, 2,2′-azobisisobutyronitrile.

attributed to CS. The carbonyl -COO absorbance at 1726 $cm^{-1}$ was assigned to PCL. The $^{1}$H-NMR spectrum was used to measure the PCL composition of CSMA-g-PCL. Peak A in Figure 1B was attributed to two protons of PCL. The sugar protons attributed to the C1 position of CSMA appeared at 4.4 ppm (Peak B). The peak intensity ratio between Peak A and Peak B was used to calculate the PCL composition of CSMA-g-PCL, that is, 7.5 mol%. Since the signals of the CSMA double bonds still appeared in CSMA-g-PCL, the residual amount of the nonreacted double bonds could be calculated from the peak intensity ratio between Peak C attributed to two protons on the double bonds of CSMA and Peak B attributed to the C1 sugar protons. A value of 31.0 mol% was obtained. Therefore, the x, y, and z values in Figure 1B indicating the composition of the three constituent repeating units of CSMA-g-PCL were 31.0, 61.5, and 7.5 mol%, respectively. These three values were utilized to calculate the PCL wt% of CSMA-g-PCL, ie, 32 wt%. This value was close to the value of 27 wt% characterized by FTIR in our previous study.[18] When a hydrophobic amount was in the range of 20–30 wt%, a micellar conformation was commonly reported.[1] The 31 mol% of the nonreacted methacrylate groups left in CSMA-g-PCL could be used to link biomolecular ligands targeting specific cells or tissues for enhanced drug delivery in future studies.

## Micellar properties and drug encapsulation

Since the amphiphilic copolymers were more hydrophobic, they could be assembled through a simple dialysis method to form micelles in an aqueous solution due to the segregation between the hydrophobic and hydrophilic segments.[22] The CMC value of CSMA-g-PCL was 5.7 μg/mL determined using pyrene as a fluorescent probe (Supplemental Figure S2).

The hydrodynamic diameters of CSMA-g-PCL without (Micelle) and with DOX (Micelle DOX) were 292.7 ± 1.9 nm (particle dispersity index [PDI] = 0.16 ± 0.11) and 350.8 ± 0.8 nm (PDI = 0.13 ± 0.02), respectively. Their corresponding zeta potentials were −27.4 ± 3.8 mV and −17.4 ± 2.1 mV (Supplemental Figure S3). The less

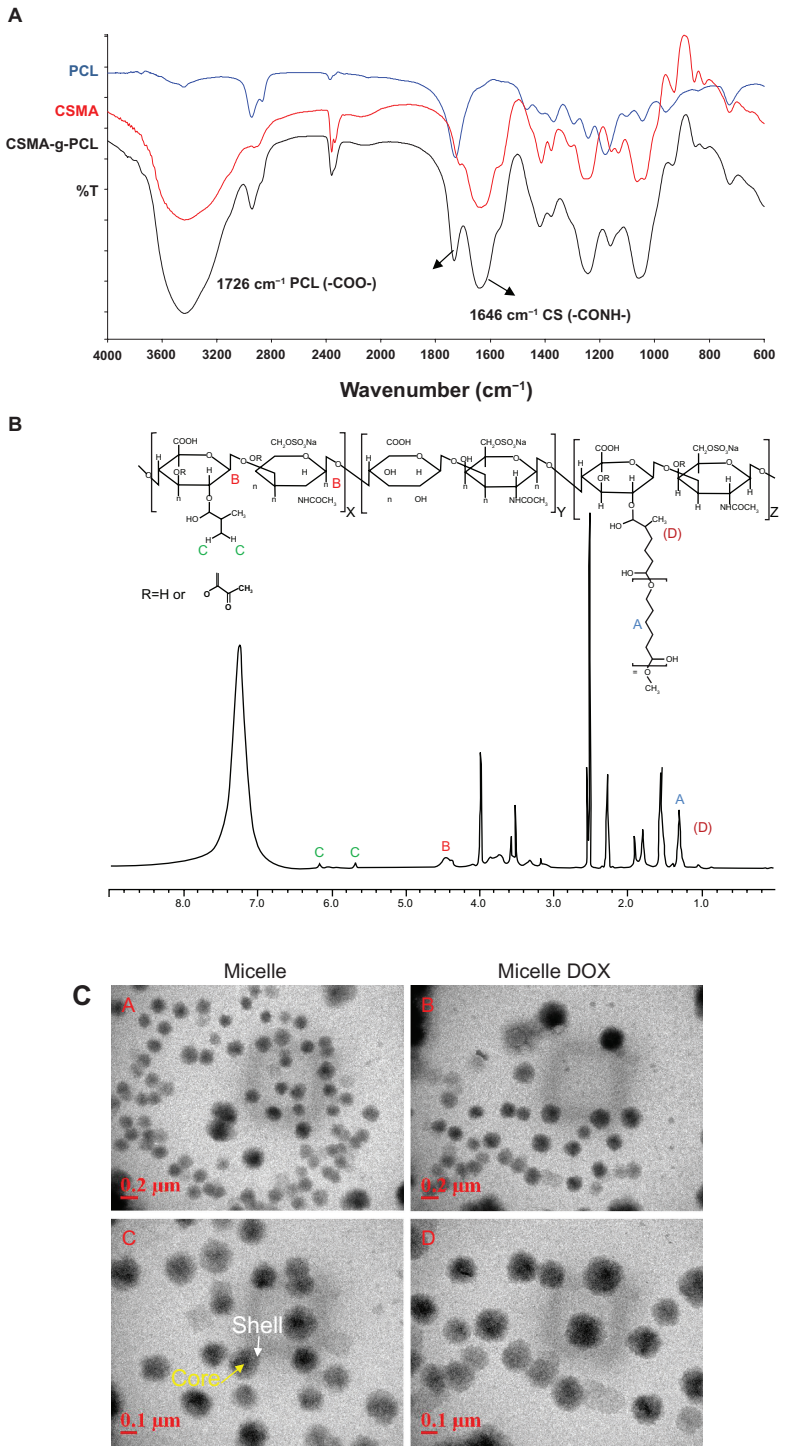


**Figure 1** (**A**) FTIR spectra of PCL, CSMA, and CSMA-*g*-PCL. (**B**) $^{1}$H-NMR spectrum of CSMA-*g*-PCL. Peak A is attributed to two protons of PCL, Peak B to the sugar protons at the C1 position of CSMA, and Peak C to the protons on the nonreacted double bonds of CSMA. (**C**) TEM images of CSMA-*g*-PCL with (Micelle DOX) and without DOX (Micelle).

**Abbreviations:** FTIR, Fourier transform infrared spectrometer; NMR, Nuclear magnetic resonance spectrometry; PCL, Poly(ε-caprolactone); CSMA, Methacrylated chondroitin sulfate; CSMA-*g*-PCL, Poly(ε-caprolactone)-*g*-methacrylated chondroitin sulfate; DOX, Doxorubicin.

negative value in zeta potential after DOX loading was due to CS being an anionic polysaccharide, which might attract DOX molecules and lead to the shielding of some negative charges on the exterior surface of CSMA-g-PCL. The morphology of the self-assembled CSMA-g-PCL was also examined by TEM as a spherical structure shown in Figure 1C. It was apparent that the hydrophobic PCL segments were assembled in the micelle core and the hydrophilic CS

backbone was exposed to the shell. The average particle sizes from 20 particles were 203 ± 5.8 nm and 226 ± 8.4 nm, respectively, for Micelle and Micelle DOX. Since the TEM samples were done in a dehydrated state and those of DLS were in a solution, the larger particle diameters of the micelles observed in DLS could be attributed to the swelling behavior of the shell compartment.[23]

The various concentrations of ε-caprolactone grafted onto chitosan from a molar ratio of 8/1 to 24/1 increased the hydrodynamic diameters from 47 to 113 nm.[24] The micellar particle size increased with an increase in the PCL segments; however, all values are smaller than that of CSMA-g-PCL. The discrepancy in particle diameter of about twofold between CSMA-g-PCL and chitosan-g-PCL might be due to the superior water solubility of CS to that of chitosan, leading to the greater swelling in the shell.

The DOX-loading efficiency of Micelle DOX was 3.60% ± 1.02% (n = 4). In vitro DOX release from Micelle DOX was carried out in 0.1 M PBS at a pH value of 6.2 or 7.4 at 37°C. As seen in Figure 2A, about 80% of the DOX was released at pH = 6.2 and 70% at pH = 7.4 in the initial 10 hours. Though the DOX base form was prepared by mixing the DOX. HCl salt in DMSO containing 3 M excess of TEA to encapsulate DOX in its hydrophobic PCL core of CSMA-g-PCL, during the dialysis process, a portion of the DOX molecules might recover to protonate the amino groups and form electrostatic interactions with CSMA-g-PCL. This fact also resulted in an increase in the zeta potential from –27.4 ± 3.8 mV to –17.4 ± 2.1 mV after DOX loading. The electrostatic interactions between the DOX molecules and CSMA-g-PCL on the exterior surface resulted in a rapid release of DOX from Micelle DOX. Since the solubility of DOX is better in acidic conditions than a neutral one, the faster release of DOX was observed in pH = 6.2 solution.[25] The pH-dependent release behavior benefits tumor-targeted DOX delivery because the solid tumor site has a pH value lower than normal tissue.[26]

## Cytotoxicity and intracellular uptake

To test which non-small-cell lung cancer cells are sensitive to DOX formulation, CL1–5, H928, NCI-H520, NCI-H358, and CRL-5802 cells exposed to Micelle DOX at various concentrations were studied. The concentrations inhibiting 50% of cell proliferation ($IC_{50}$) values were 1.55 μg/mL, 0.77 μg/mL, 0.82 μg/mL, 0.08 μg/mL, and 0.53 μg/mL in the cell order, respectively (Figure 2B). Micelle DOX showed the best cell-killing ability against NCI-H358 cells. This cell line along with CRL-5802 was selected for a more detailed study of cell viability after exposure to the copolymer itself.

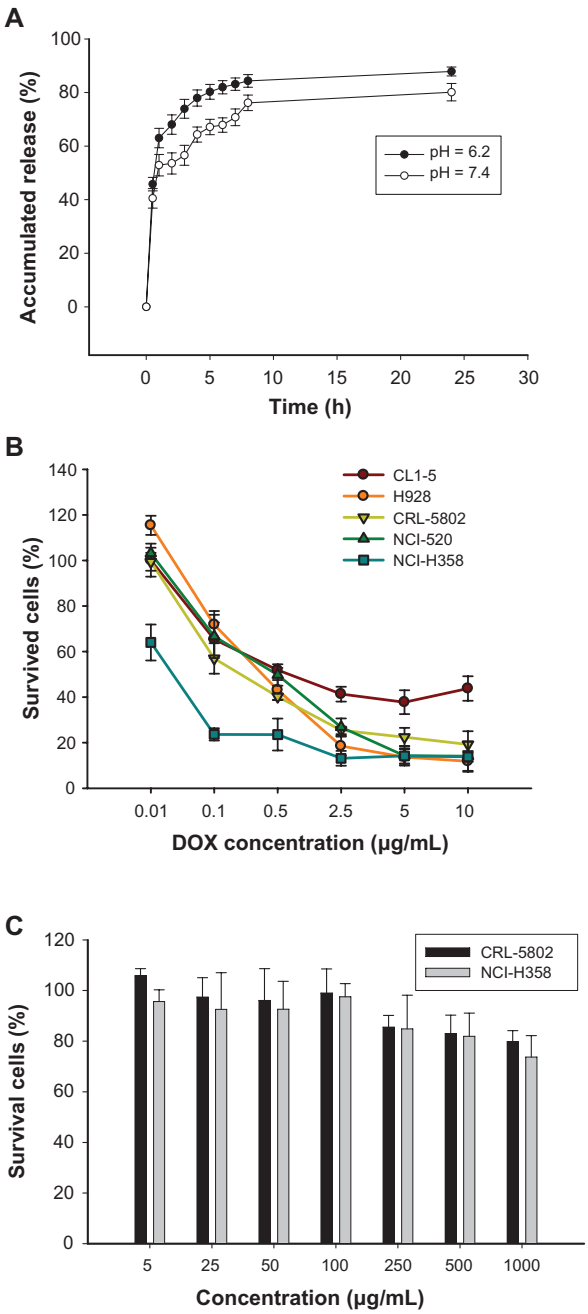


**Figure 2** (**A**) In vitro DOX release from Micelle DOX carried out in 0.1 M PBS at pH = 6.2 or 7.4 at 37°C (n = 4). (**B**) Cell viability of five non-small-cell lung cancer cells exposed to Micelle DOX at various DOX concentrations. (**C**) Cell viability of CRL-5802 and NCI-H358 exposed to CSMA-g-PCL (n = 8).
**Abbreviations:** DOX, Doxorubicin; PBS, Phosphate-buffered saline; CSMA-g-PCL, Poly(ε-caprolactone)-g-methacrylated chondroitin sulfate.

Cytotoxic studies as determined by MTT assay demonstrated CRL-5802 and NCI-H358 cells incubated with CSMA-g-PCL at a concentration of less than 100 μg/mL remained ~100% viable (Figure 2C). Cytotoxicity was slightly dose-dependent on the CSMA-g-PCL concentration.

To examine the antitumor potency of DOX-loaded nanoparticles, the cells were exposed to free DOX or Micelle DOX

at various concentrations for 24 hours. A commercial product, Lipo DOX, was chosen as a positive control group. However, the cell-killing ability was insensitive to increasing Lipo DOX concentration in both NCI-H358 and CRL-5802 cells because DOX cannot easily be released from the inner acidic environment (Supplemental Figure S4). The $IC_{50}$ values in CRL-5802 cells were 0.76 μg/mL for free DOX and 5.1 μg/mL for Micelle DOX. In NCI-H358 cells, the $IC_{50}$ values were 1.35 μg/mL and 0.22 μg/mL corresponding to free DOX and Micelle DOX, respectively.

Flow cytometric analysis was utilized to study the intracellular uptake of free DOX, Lipo DOX, and Micelle DOX into CRL-5802 and NCI-H358 cells at various time points using an equivalent DOX concentration of 0.5 μg/mL. A greater shift to the right corresponds to the large amount of DOX internalized into the cells. The largest shift was observed in Micelle DOX in both cell lines (Figure 3). Clearly, in CRL-5802 cells, 3 hours of incubation was sufficient to optimize the cellular internalization for free DOX and Micelle DOX while in NCI-H358 cells, the cellular internalization gradually increased with time.

The high fluorescence intensity observed by flow cytometry might not correlate with therapeutic efficacy if DOX does not penetrate the site of action of the cell nuclei. Thus, a further comparison of cellular internalization between free DOX and Micelle DOX was carried out using CLSM. As seen in Figure 4A, Micelle DOX could enter into the cytoplasm of CRL-5802 cells after 3 hours of incubation. In contrast, for the cells incubated with free DOX, strong fluorescence was observed in the cell nuclei when the cells were incubated after 3 hours and this strengthened after 24 hours of incubation. On the other hand, CLSM images in NCI-H358 cells showed both DOX and Micelle DOX emitted high fluorescence intensity in

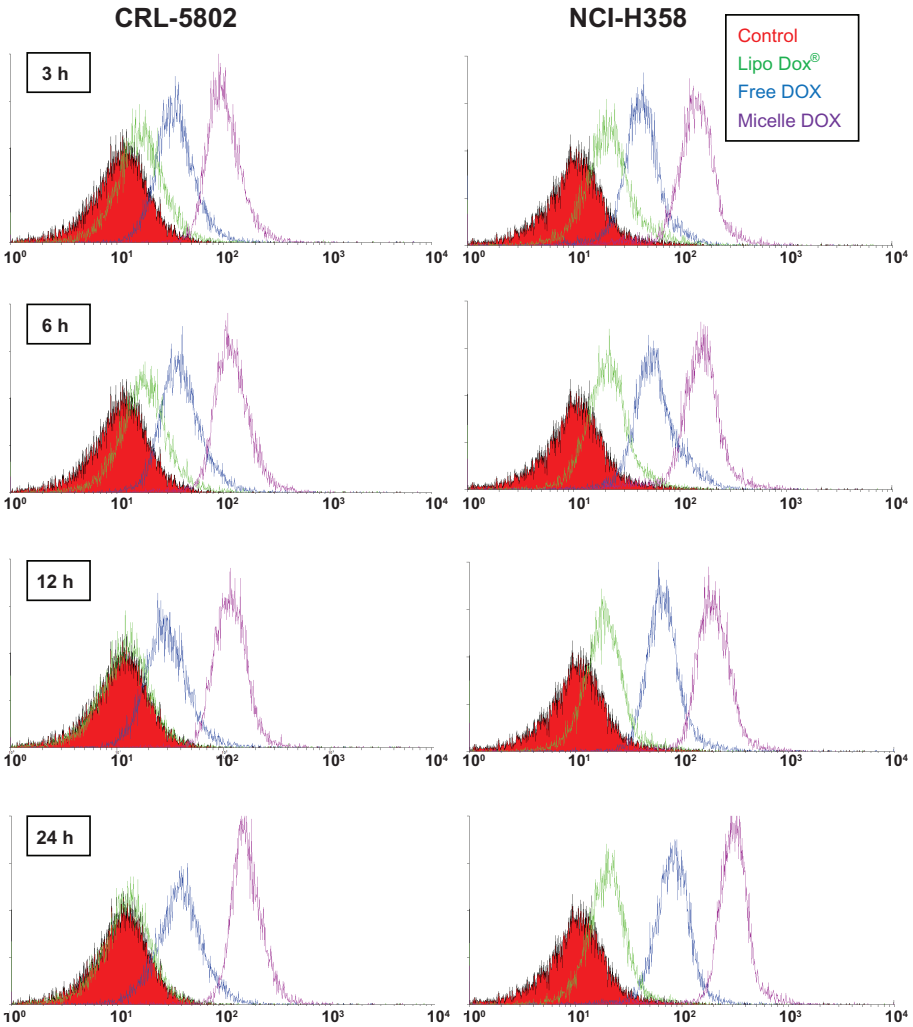


**Figure 3** Flow cytometric histograms of CRL-5802 and NCI-H358-internalized DOX (blue), Lipo DOX (green), and Micelle DOX (purple) relative to the control cells at different incubation time points. Free DOX, Lipo DOX®, and Micelle DOX was tested at an equivalent DOX concentration of 0.5 μg/mL.
**Abbreviations:** DOX, Doxorubicin; Lipo DOX, Doxorubicin-encapsulated liposome.

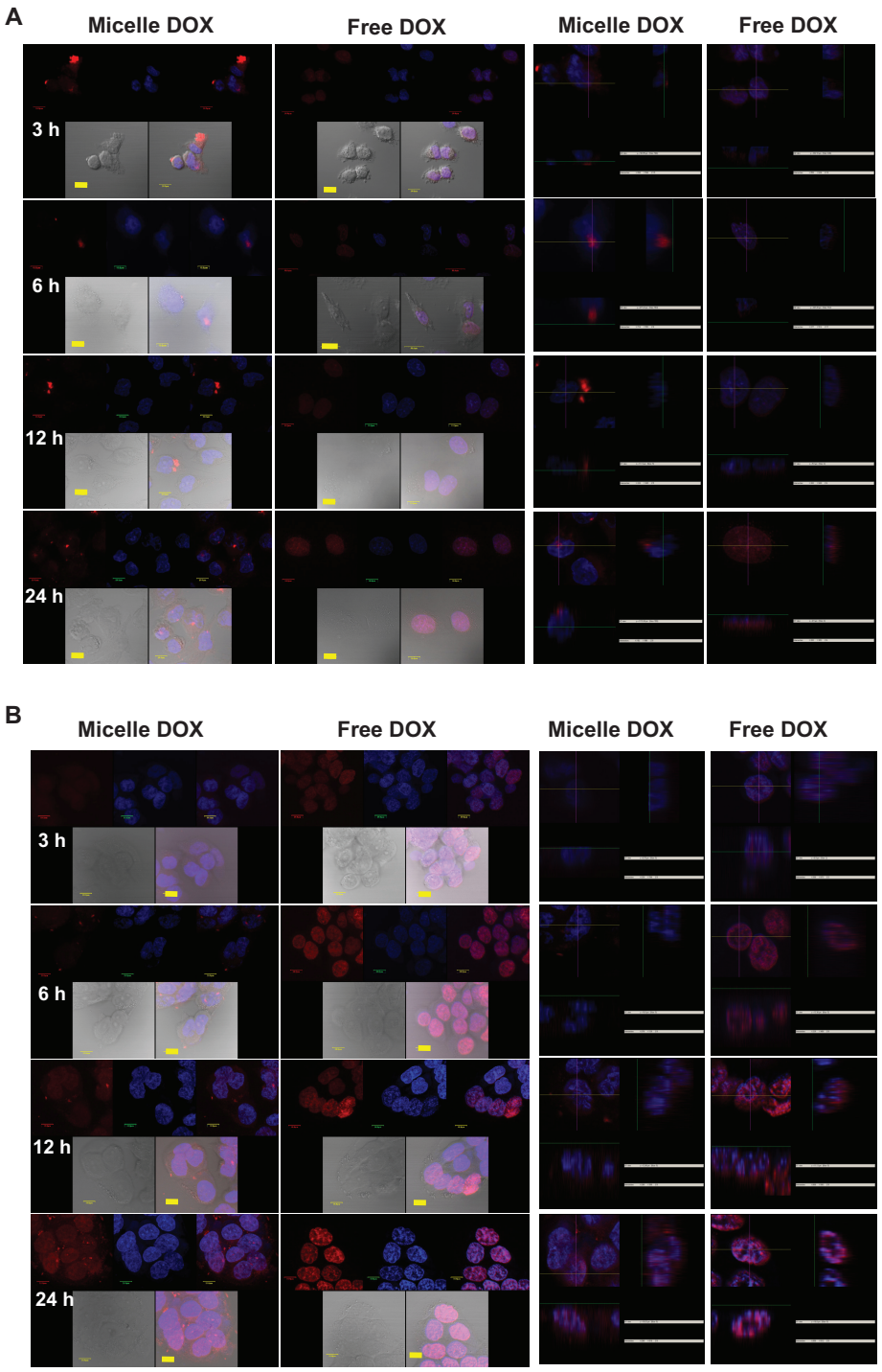


**Figure 4** Confocal microscopic photographs of (**A**) CRL-5802, and (**B**) NCI-H358 internalized free DOX, and Micelle DOX at different incubation time periods (1 bar = 10 μm).
**Notes:** Column 1 is Micelle DOX. Column 2 is free DOX. Column 3 is the z-section image of Micelle DOX. Column 4 is the z-section image of free DOX. The red color is DOX; the blue color is DAPI-stained cell nuclei, and the purple color represents a merged image of both.
**Abbreviations:** DOX, Doxorubicin; DAPI, 4',6-diamidino-2-phenylindole.

contrast with CRL-5802 cells in all four incubation periods, suggesting NCI-H358 cells could internalize the free or formulated DOX more efficiently than CRL-5802 cells (Figure 4B). This result implied CSMA-g-PCL was an efficient drug carrier to deliver DOX into the cytoplasm, but took time to transport DOX into the nuclei to perform its action. The preferential internalization in NCI-H358 cells compared with CRL-5802 cells was suspected to be the reason for the different vasculature or CD44 receptor densities in the two types of cells.

The superior NCI-H358 cell-killing ability using Micelle DOX compared with free DOX might be explained by two possible mechanisms. Mohan and Rapoport[27] have pointed out that the deprotonation of DOX to increase encapsulation efficiency in hydrophobic micelle cores would hinder the penetration of DOX into the cell nuclei. Thus, reprotonation of DOX in acidic organelles (such as endosomes, lysosomes) could improve the cell-killing ability of the drug. The electrostatic interactions between the positively-charged DOX molecules and the negatively-charged CSMA-g-PCL on the exterior surface resulted in a rapid release of DOX from the Micelle DOX. The second possible explanation for the high cell-killing efficiency in the Micelle DOX was that the micellar particles are usually internalized inside cells by endocytosis, while free drugs mainly do this by diffusion.[28] Using the endocytosis mechanism to facilitate a cellular internalization has been widely reported in amphiphilic copolymers prepared by either block[25,29] or graft copolymerization,[12,13] which could increase drug availability in the cytoplasm. Optimizing the drug release from drug-encapsulated nanoparticles after entering inside cells is also a key factor to designing a successful drug delivery system. Thus, a main advantage of CSMA-g-PCL as a DOX carrier is that both CS and PCL are biodegradable due to the susceptibility of aliphatic ester and sugar linkages, especially in low pH environments, where the DOX molecules are sequentially released and perform an action.

## In vivo biodistribution and antitumor activity

To evaluate the in vivo uptake of CSMA-g-PCL, the biodistribution of IR-780-loaded CSMA-g-PCL was studied in nude mice. We optically imaged the IR-780 intensity in CRL-5802 and NCI-H358 tumor-bearing mice at different time points. The fluorescence intensity of IR-780 increased with increasing circulation time of the IR-780-loaded micelles in

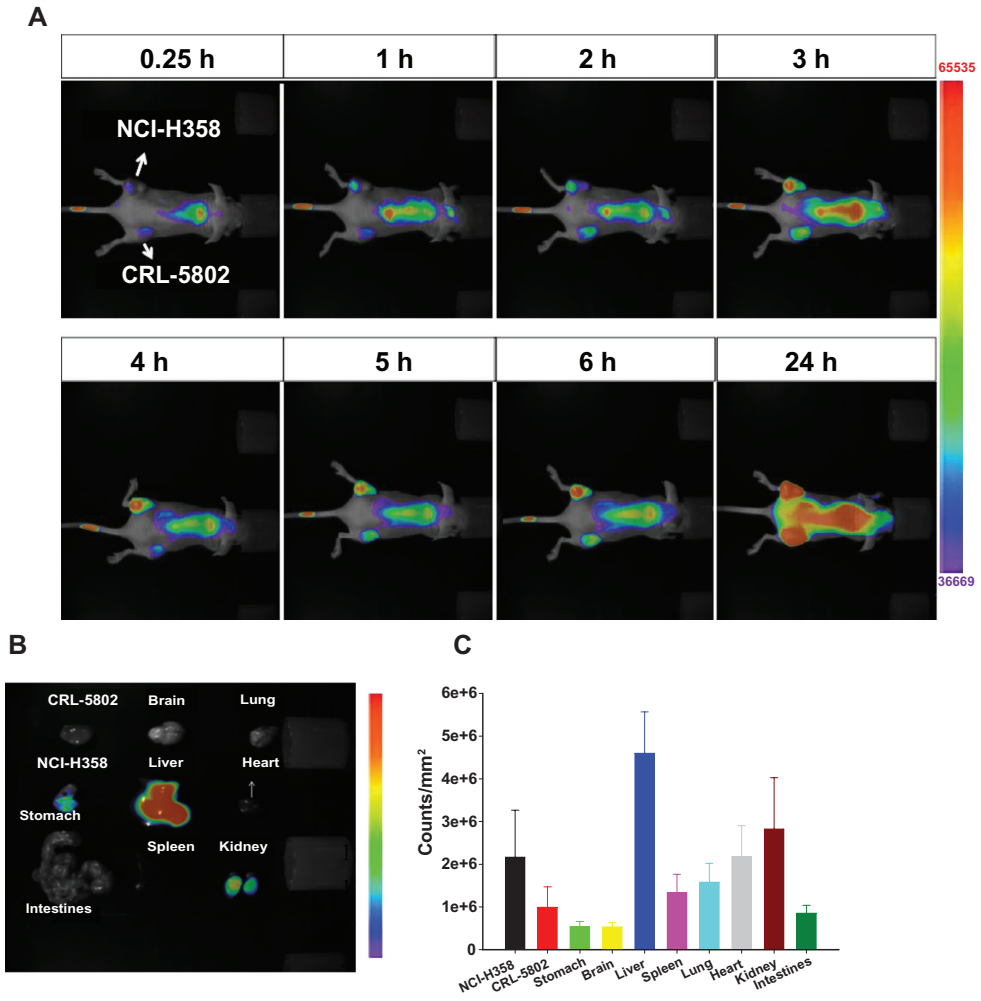


**Figure 5** (**A**) Biodistribution in female Balb/c mice (6–8 weeks old) using a near-infrared noninvasive optical imaging technique. (**B**) Isolated tissues and (**C**) their relative fluorescent intensities after the mice were injected with IR-780-loaded CSMA-g-PCL micelle for 24 hours using an optical image system (n = 5).
**Abbreviation:** CSMA-g-PCL, Poly(ε-caprolactone)-g-methacrylated chondroitin sulfate.

the mice (Figure 5). The relevant organs, tissues, and tumors were dissected from the mice at 24 hours after instillation and imaged immediately to determine biodistribution. Fluorescence emission was normalized to pixel counts per millimeter squared (counts/mm$^2$). Most of the micelles were taken up by the RES such as the liver, and the fluorescence intensity in the NCI-H358 tumor was higher than that in CRL-5802. This finding was consistent with the result in the cellular uptake study conducted using a flow cytometer and a CLSM. The NCI-H358 cells had better cellular uptake of Micelle DOX than the CRL-5802 cells, leading to the lower $IC_{50}$ value. Next, a long accumulation of IR-780-loaded CSMA-g-PCL was studied in NCI-H358 tumor-bearing mice. In Figure 6, at 96 hours after tail-vein injection of the IR-780-loaded micelles into the mice, we still observed IR-780 fluorescence at the tumor site because of the immature lymphatic drainage system of the tumor tissues. This enhanced permeability and retention (EPR) effect[30] in tumors increased the efficacy of using nanoformulated drugs to treat cancer diseases as compared with their free drugs.

The in vivo therapeutic efficacy of Micelle DOX was also examined in the NCI-H358 tumor-bearing mouse model. When tumor sizes reached approximately 150 mm$^3$, DOX or Micelle DOX was intravenously injected via the lateral tail vein at a single dose of 5 mg DOX per kg of animal weight. PBS was used as a control group. The sizes of the subcutaneous tumors were measured every 2 days over 42 days. Within the first 10 days, the tumor sizes of the treated groups did not show a statistically significant difference from the control group. After that, the tumors in the PBS group rapidly increased (Figure 7A). The Micelle DOX-treated group showed a greater inhibition in tumor growth than the free DOX-treated group. On day 30, after treatment with Micelle DOX, the tumor growth was significantly inhibited ($P < 0.05$) when compared with those received by PBS or DOX. The mean tumor volume increase at this time point was 14-, 8.5-, and 4.5-fold for the mice treated with PBS, DOX, and Micelle DOX, respectively. Figure 7B shows the optical images of tumors dissected from the mice on day 42. Tumors with serious necrosis were observed in the mice treated with PBS or DOX, but none appeared in those treated with Micelle DOX. To evaluate the toxicity of the Micelle DOX formulation, we also measured the body weight of the mice in each cohort. It was apparent none of the three formulations showed any decrease in the body weight of the mice (Figure 7C) and no mouse died during the 42-day study. Because of the EPR effect[30] in tumor tissues, the in vivo treatment of the mice bearing the NCI-H358 tumor with Micelle DOX showed better tumor suppression than those treated with free DOX using a single dose of 5 mg/kg.

## Conclusions

The PCL molar percent of the CSMA-g-PCL copolymer was calculated from the $^1$H-NMR spectrum, ie, 7.5 mol%, resulting in a micellar structure. DOX was successfully loaded into the CSMA-g-PCL micelles through a simple dialysis method. The change in hydrodynamic diameter was trivial, but the change in zeta potential was remarkable after DOX loading. This may be due to the counter positive DOX molecules forming electrostatic interactions with the anionic

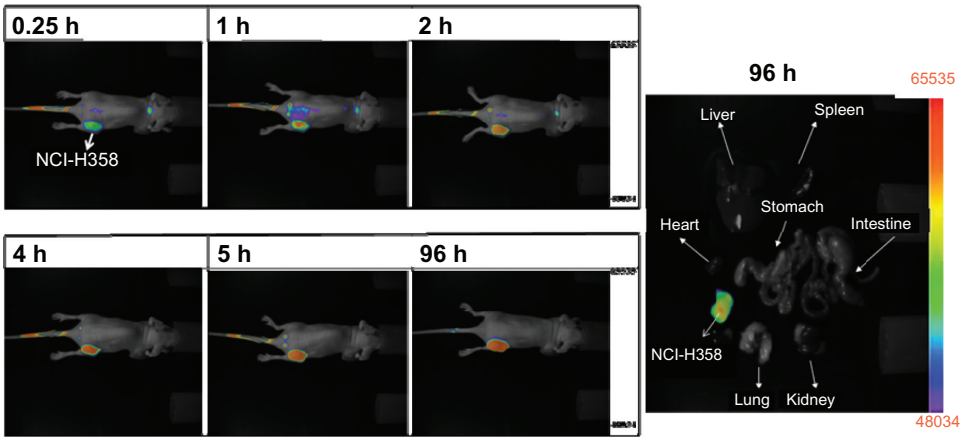


**Figure 6** NCI-H-358 tumor accumulation of IR-780-loaded CSMA-g-PCL micelle in female Balb/c mice (6–8 weeks old) according to time and isolated tissues at 96 h after instillation using a NIR non-invasive optical imaging technique (n = 3 mice).
**Abbreviation:** CSMA-g-PCL, Poly(ε-caprolactone)-g-methacrylated chondroitin sulfate.

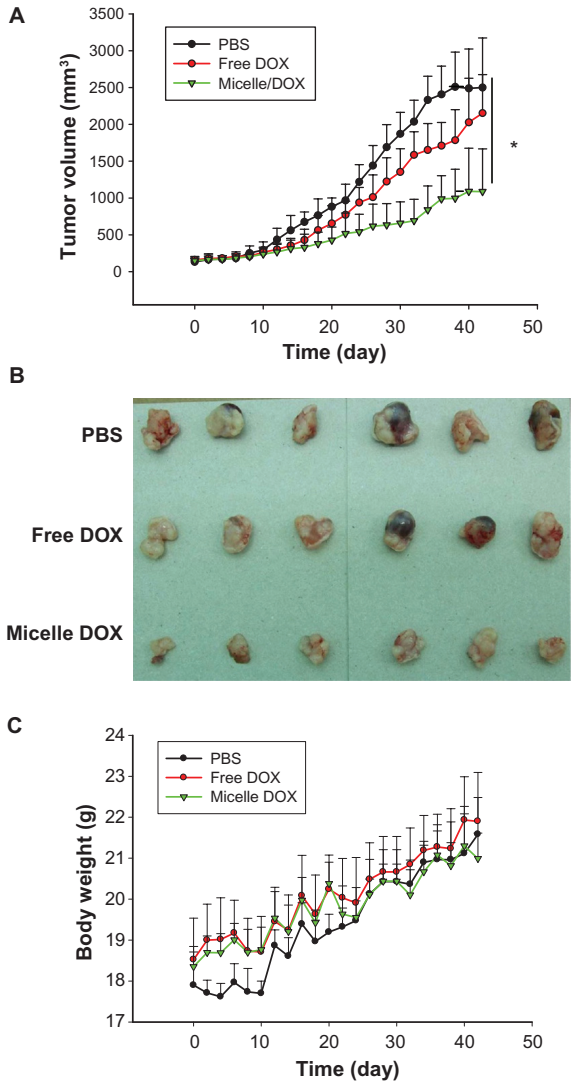


**Figure 7** In vivo antitumor efficacy of free DOX and Micelle DOX in the NCI-H358 tumor-bearing model. (**A**) Tumor volume profiles according to time. (**B**) Photographic images of tumors removed at day 42 after the mice were sacrificed. (**C**) Body weight of the mice according to time.
**Abbreviation:** DOX, Doxorubicin.

CSMA-g-PCL during dialysis. The DOX release from Micelle DOX was faster at pH = 6.2 than that at pH = 7.4. The DOX released from Micelle DOX showed better cell-killing ability than free DOX in NCI-H358 cells. This result was confirmed by a cell-based study using a flow cytometer and a CLSM as well as by a tissue-based study using a fluorescence optical imaging technique. The Micelle DOX displayed higher DOX internalization in the NCI-H358 tumor than in the CRL-5802 tumor. After intravenously injecting the mice with the NCI-H358 tumor, the Micelle DOX could be passively targeted to the tumor tissue by the EPR effect, leading to better anticancer activity compared with free DOX. Using the biodegradable CSMA-g-PCL micelles for a drug delivery system seems attractive because there is no safety concern of the carrier following drug release. A new type of amphiphilic CSMA-g-PCL copolymer was successfully prepared and its potential application as a drug carrier for anticancer agents was illustrated.

## Acknowledgments/Disclosure

We are grateful for the financial support of the National Science Council of Taiwan under grant numbers NSC 98-2320-B-037-002 and NSC 101-2325-B-037-006 and the support of the Kaohsiung Medical University Research Foundation. The authors report no conflicts of interest in this work.

## References

1. Letchford K, Burt H. A review of the formation and classification of amphiphilic block copolymer nanoparticulate structures: micelles, nanospheres, nanocapsules and polymersomes. *Eur J Pharm Biopharm*. 2007;65(3):259–269.
2. Yang YQ, Zheng LS, Guo XD, Qian Y, Zhang LJ. pH-sensitive micelles self-assembled from amphiphilic copolymer brush for delivery of poorly water-soluble drugs. *Biomacromolecules*. 2010;12(1):116–122.
3. Pourcelle V, Devouge S, Garinot M, Preat V, Marchand-Brynaert J. PCL-PEG-based nanoparticles grafted with GRGDS peptide: preparation and surface analysis by XPS. *Biomacromolecules*. 2007;8(12):3977–3983.
4. Sonaje K, Italia JL, Sharma G, Bhardwaj V, Tikoo K, Kumar MN. Development of biodegradable nanoparticles for oral delivery of ellagic acid and evaluation of their antioxidant efficacy against cyclosporine A-induced nephrotoxicity in rats. *Pharm Res*. 2007;24(5):899–908.
5. Garinot M, Fievez V, Pourcelle V, et al. PEGylated PLGA-based nanoparticles targeting M cells for oral vaccination. *J Control Release*. 2007;120(3):195–204.
6. Liu ZH, Jiao YP, Wang YF, Zhou CR, Zhang ZY. Polysaccharides-based nanoparticles as drug delivery systems. *Adv Drug Deli Rev*. 2008;60:1650–1662.
7. Lemarchand C, Couvreur P, Besnard M, Costantini D, Gref R. Novel polyester-polysaccharide nanoparticles. *Pharm Res*. 2003;20(8):1284–1292.
8. Rodrigues JS, Santos-Magalhaes NS, Coelho LC, Couvreur P, Ponchel G, Gref R. Novel core(polyester)-shell(polysaccharide) nanoparticles: protein loading and surface modification with lectins. *J Control Release*. 2003;92(1–2):103–112.
9. Lemarchand C, Gref A, Couvreur P. Polysaccharide-decorated nanoparticles. *Eur J Pharm Biopharm*. 2004;58(2):327–341.
10. Lemarchand C, Gref R, Lesieur S, et al. Physico-chemical characterization of polysaccharide-coated nanoparticles. *J Control Release*. 2005;108(1):97–111.
11. Yadav AK, Mishra P, Jain S, Mishra AK, Agrawal GP. Preparation and characterization of HA-PEG-PCL intelligent core-corona nanoparticles for delivery of doxorubicin. *J Drug Target*. 2008;16(6):464–478.
12. Pitarresi G, Palumbo FS, Albanese A, Fiorica C, Picone P, Giammona G. Self-assembled amphiphilic hyaluronic acid graft copolymers for targeted release of antitumoral drug. *J Drug Target*. 2010;18(4):264–276.
13. Wildgruber M, Lee H, Chudnovskiy A, et al. Monocyte subset dynamics in human atherosclerosis can be profiled with magnetic nano-sensors. *PLoS One*. 2009;4(5):e5663.
14. Du YZ, Weng Q, Yuan H, Hu FQ. Synthesis and antitumor activity of stearate-g-dextran micelles for intracellular doxorubicin delivery. *ACS Nano*. 2010;4(11):6894–6902.
15. Pipitone VR. Chondroprotection with chondroitin sulfate. *Drugs Exp Clin Res*. 1991;17(1):3–7.
16. Volpi N. Chondroitin sulfate for the treatment of osteoarthritis. *Curr Med Chem Anti Inflamm Anti Allergy Agents*. 2005;4(3):221–234.

17. Wang LF, Shen SS, Lu SC. Synthesis and characterization of chondroitin sulfate-methacrylate hydrogels. *Carbohy Polym*. 2003;52(7):389–396.
18. Chen AL, Ni HC, Wang LF, Chen JS. Biodegradable amphiphilic copolymers based on poly(epsilon-caprolactone)-graft chondroitin sulfate as drug carriers. *Biomacromolecules*. 2008;9(9):2447–2457.
19. Wang LF, Ni HC, Lin CC. Chondroitin sulfate-g-poly(varepsilon-caprolactone) co-polymer aggregates as potential targeting drug carriers. *J Biomater Sci Polym Ed*. September 22, 2011. [Epub ahead of print.]
20. Mosmann T. Rapid colorimetric assay for cellular growth and survival: application to proliferation and cytotoxicity assays. *J Immunol Methods*. 1983;65(1–2):55–63.
21. Wang LL, Zhang Z, Li Q, et al. Ethanol exposure induces differential microRNA and target gene expression and teratogenic effects which can be suppressed by folic acid supplementation. *Hum Reprod*. 2009;24(3):562–579.
22. Allen C, Maysinger D, Eisenberg A. Nano-engineering block copolymer aggregates for drug delivery. *Colloid Surf B Biointerfaces*. 1999;19(1–4):3–27.
23. Bodnar M, Hartmann JF, Borbely J. Synthesis and study of cross-linked chitosan-N-poly(ethylene glycol) nanoparticles. *Biomacromolecules*. 2006;7(11):3030–3036.
24. Duan K, Zhang X, Tang X, et al. Fabrication of cationic nanomicelle from chitosan-graft-polycaprolactone as the carrier of 7-ethyl-10-hydroxy-camptothecin. *Colloid Surf B Biointerfaces*. 2010;76(2):475–482.
25. Shuai X, Ai H, Nasongkla N, Kim S, Gao J. Micellar carriers based on block copolymers of poly(epsilon-caprolactone) and poly(ethylene glycol) for doxorubicin delivery. *J Control Release*. 2004;98(3):415–426.
26. Breunig M, Bauer S, Goepferich A. Polymers and nanoparticles: intelligent tools for intracellular targeting? *Eur J Pharm Biopharm*. 2008;68(1):112–128.
27. Mohan P, Rapoport N. Doxorubicin as a molecular nanotheranostic agent: effect of doxorubicin encapsulation in micelles or nanoemulsions on the ultrasound-mediated intracellular delivery and nuclear trafficking. *Mol Pharm*. 2010;7(6):1959–1973.
28. Nishiyama N, Kataoka K. Nanostructured devices based on block copolymer assemblies for drug delivery: designing structures for enhanced drug function. *Adv Polym Sci*. 2006;193:67–101.
29. Xiong XB, Ma Z, Lai R, Lavasanifar A. The therapeutic response to multifunctional polymeric nano-conjugates in the targeted cellular and subcellular delivery of doxorubicin. *Biomaterials*. 2010;31(4):757–768.
30. Maeda H, Matsumura Y. EPR effect based drug design and clinical outlook for enhanced cancer chemotherapy. *Adv Drug Deliv Rev*. 2011;63(3):129–130.

# Supplementary figures

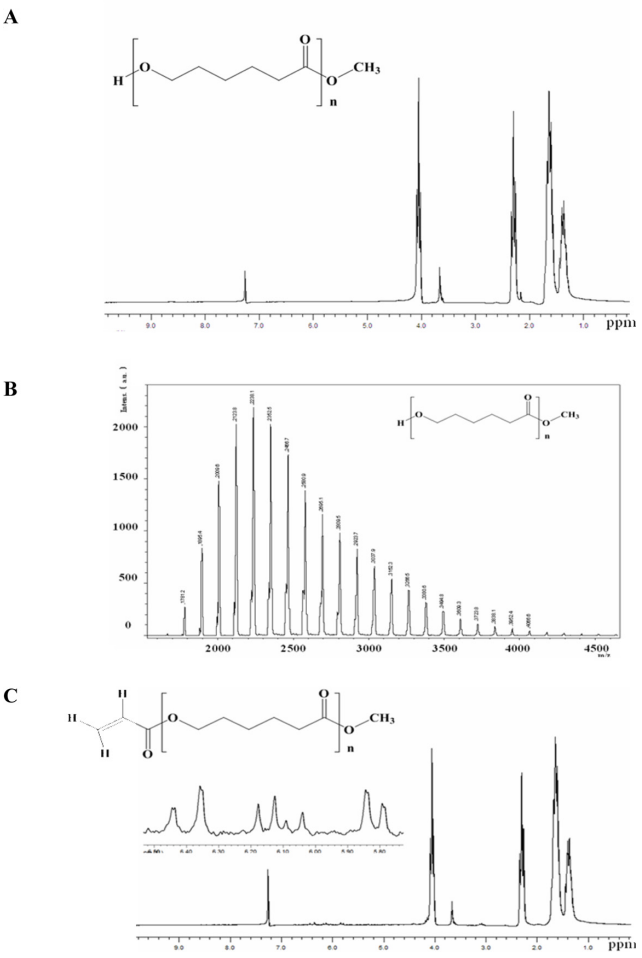


**Figure S1** (**A**) $^1$H-NMR and (**B**) MALDI-MS of MeO-PCL-OH; (**C**) $^1$H-NMR of MeO-PCL-AC.

**Abbreviations:** NMR, Nuclear magnetic resonance; MALDI-MS, matrix-assisted laser desorption/ionization-mass spectrometry; MeO-PCL-OH, Methoxy-capped poly(ε-caprolactone); MeO-PCL-Ac, Methoxy-capped poly(ε-caprolactone) acrylate.

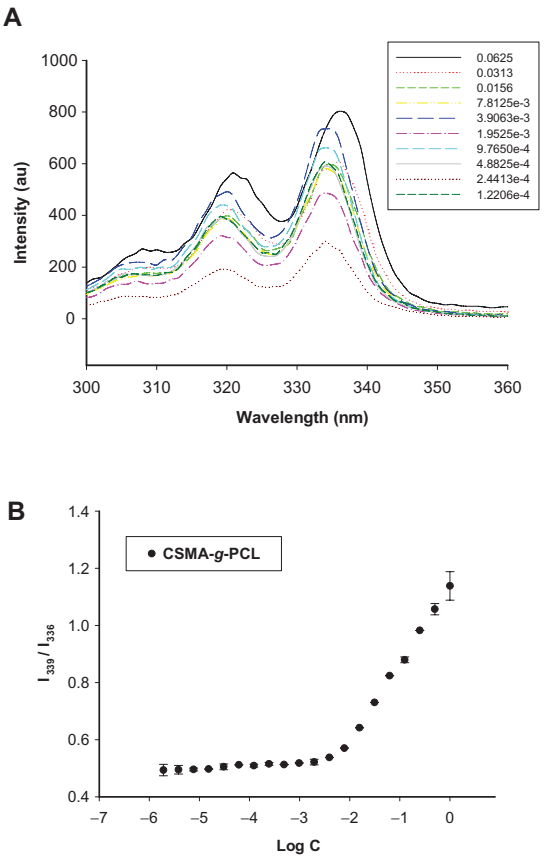


**Figure S2** Critical micelle concentration measurement of CSMA-g-PCL using pyrene as a probe.

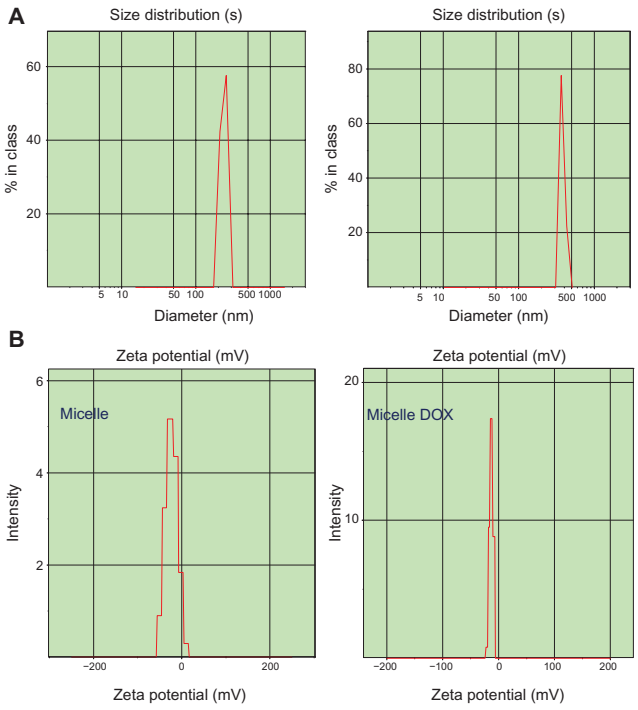


**Figure S3** (**A**) DLS histograms and (**B**) zeta potentials of CSMA-g-PCL with DOX (Micelle DOX) or without DOX (Micelle).

**Abbreviations:** DSL, Dynamic light scattering; CSMA-g-PCL, Poly(ε-caprolactone)-g-methacrylated chondroitin sulfate; DOX, Doxorubicin.

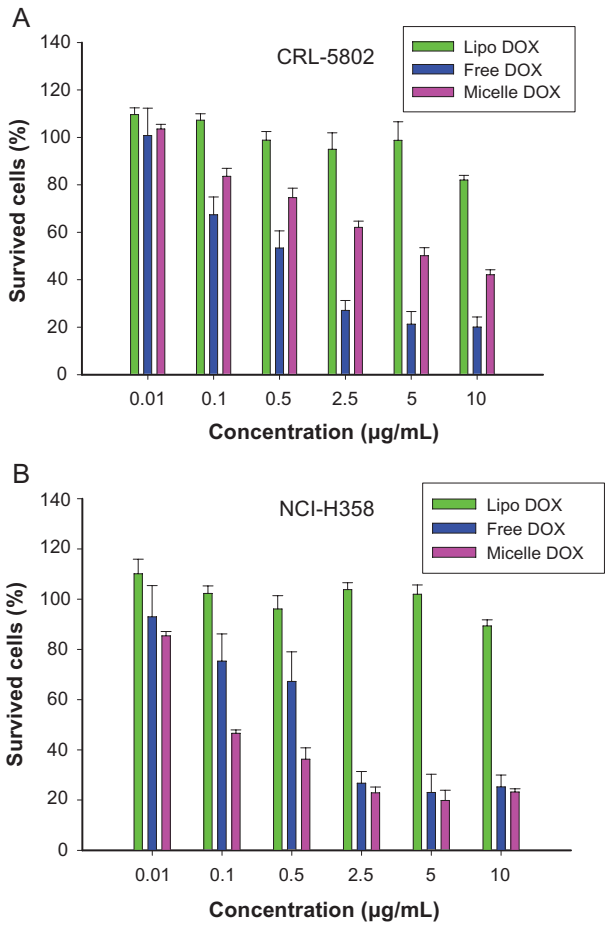


**Figure S4** Cell viability of (**A**) CRL-5802 and (**B**) NCI-H358 cells exposed to free DOX, DOX-loaded liposome (Lipo DOX), and DOX-loaded CSMA-g-PCL ( Micelle DOX) for 24 hours (n = 8).

**Abbreviations:** DOX, Doxorubicin; Lipo DOX, Doxorubicin-encapsulated liposome; CSMA-g-PCL, Poly(ε-caprolactone)-g-methacrylated chondroitin sulfate.